

Production and Properties of Highly Oriented Polyoxymethylene by Die-Drawing

A. K. Taraiya,¹ M. S. Mirza,² J. Mohanraj,¹ D. C. Barton,² I. M. Ward¹

¹Department of Physics and Astronomy, University of Leeds, Leeds LS2 9JT, United Kingdom

²School of Mechanical Engineering, University of Leeds, Leeds LS2 9JT, United Kingdom

Received 8 February 2002; accepted 7 June 2002

Published online 19 February 2003 in Wiley InterScience (www.interscience.wiley.com). DOI 10.1002/app.11848

ABSTRACT: Highly oriented monofilaments were produced by a high-temperature die-drawing process followed by tensile drawing. It was shown that a successful high-speed process required high-quality melt-extruded rod. The mechanical properties and structure of the die-drawn products were investigated by means of tensile and bending tests, dynamic mechanical measurements, DSC, and X-ray diffraction. The bending modulus and the tensile strength increased with increasing draw ratio. It was also observed

that at high draw ratios the γ -dispersion peak in the dynamic mechanical $\tan \delta$ curve, which is associated with main chain micro-Brownian motion in the amorphous regions, diminishes, implying that these chains become taut. © 2003 Wiley Periodicals, Inc. *J Appl Polym Sci* 88: 1268–1278, 2003

Key words: oriented polymers; die-drawing; mechanical properties; polyoxymethylene; chain

INTRODUCTION

It is well known that the mechanical properties of isotropic polymers, such as tensile modulus and tensile strength, can be considerably improved by orientation of the molecular chains.^{1–4} This can be achieved by deforming the polymer in the solid state, and die-drawing is one of the techniques that has become established as a solid-state polymer deformation process.^{5–10} In this process a heated polymer billet is drawn through a heated die by applying a pulling force on the billet at the exit side. Initial die-drawing work at Leeds University was carried out on a small-scale batch die-drawing facility and, for polypropylene, has been successfully scaled up to a continuous commercially viable process.¹¹

Polyoxymethylene (POM) has previously been oriented by various methods such as tensile drawing, hydrostatic extrusion, and die-drawing to give high modulus and high strength.^{12–15} The aim of this work was to study the die-drawing behavior of POM, which is known to exhibit high stiffness, tensile strength, creep resistance, and fatigue endurance. A specific related objective was to develop a continuous process for the production of highly oriented POM.

EXPERIMENTAL

Materials

This investigation was started with a grade of commercially available POM, DuPont Delrin 150SA. Recently, this grade was replaced by Delrin 7031, which contains an additive for improved processability. Both of these grades are homopolymers with number-average molecular weight of about 66,000 and polydispersity of 2. Commercially extruded rods of Delrin 150SA (10.3 mm diameter) and Delrin 7031 (5.3 mm diameter) were supplied by DuPont (U.K.) (Hemel Hempstead, Hertfordshire, UK).

Die drawing

The die-drawing experiments were performed on the large-scale die-drawing machine described in a previous publication.¹⁶

Conical steel dies of semiangle 5, 10, 15, and 20° were used. Before each run, a billet was placed within the die so that the tag protruded through it, and the draw grips were attached. The billet was heated for approximately 1 h at the prescribed draw temperature to reach thermal equilibrium. The drawing process was then started at a low speed, usually 10 mm/min. To study the effect of draw speed on the draw ratio and the draw load, it was necessary to increase the draw speed several times during each drawing run. Product diameter and draw load were recorded under steady-state conditions. The drawing speed was continuously increased in steps until the product frac-

Correspondence to: I. M. Ward (i.m.ward@leeds.ac.uk).

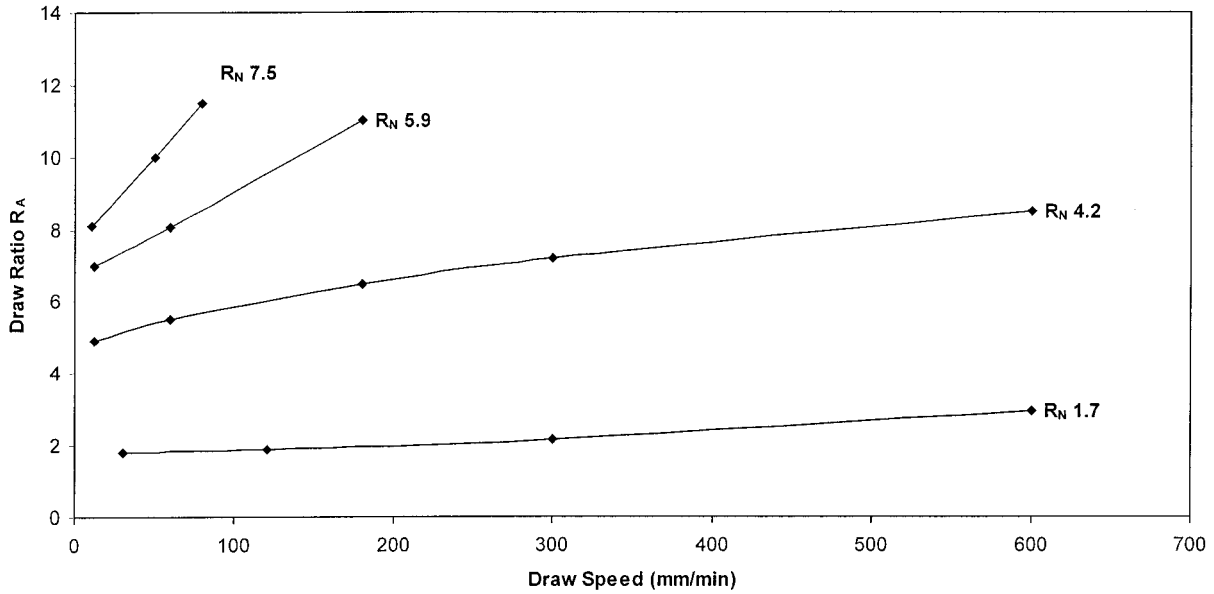


Figure 1 Variation of draw ratio R_A with draw speed for Delrin 150SA at draw temperature 160°C.

tured, or up to the maximum limiting speed allowed on the machine. In all cases, the nominal draw ratio R_N and the actual draw ratio R_A were used to quantify the drawing behavior and these quantities are defined by

$$R_N = \frac{\text{Original billet cross - section area}}{\text{Die exit cross - section area}}$$

$$R_A = \frac{\text{Original billet cross - section area}}{\text{Final product cross - section area}}$$

and the draw stress is given by

$$\sigma = \frac{\text{Draw load}}{\text{Final product cross - section area}}$$

Characterization

Only the Delrin 150SA samples drawn at 160°C to different draw ratios were characterized in this study. The bending modulus was measured at 20°C, using an Instron machine equipped with a compression load cell and a three-point bend rig. This type of test was preferred to tensile tests because of the measuring accuracy and the fact that no sample gripping damage

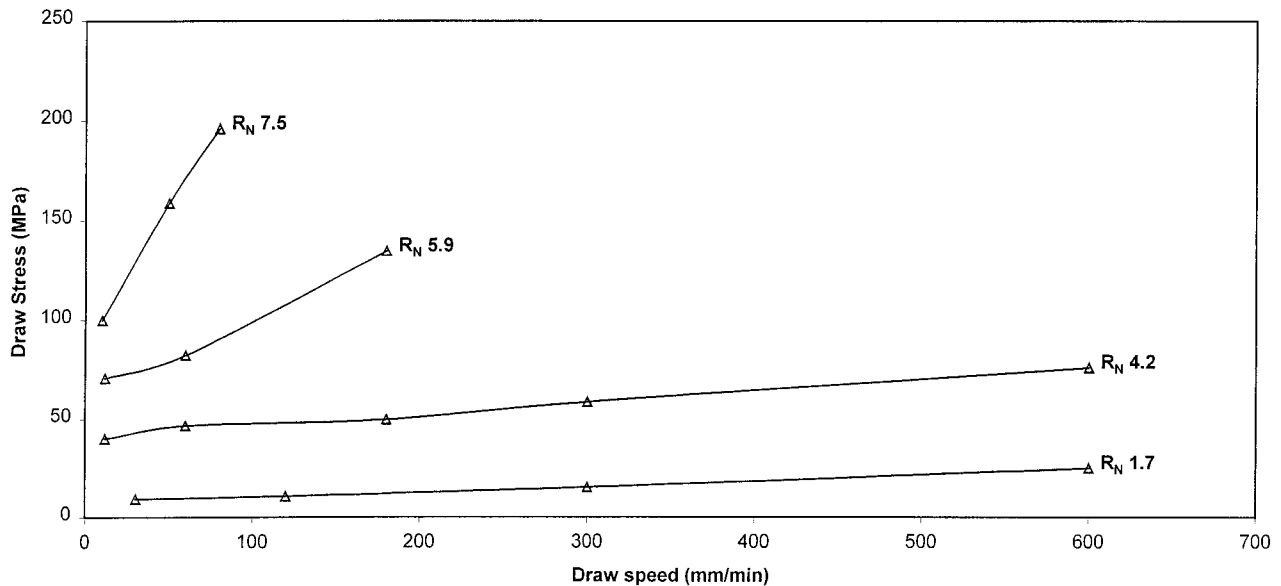


Figure 2 Variation of draw stress with draw speed for Delrin 150SA at draw temperature 160°C.

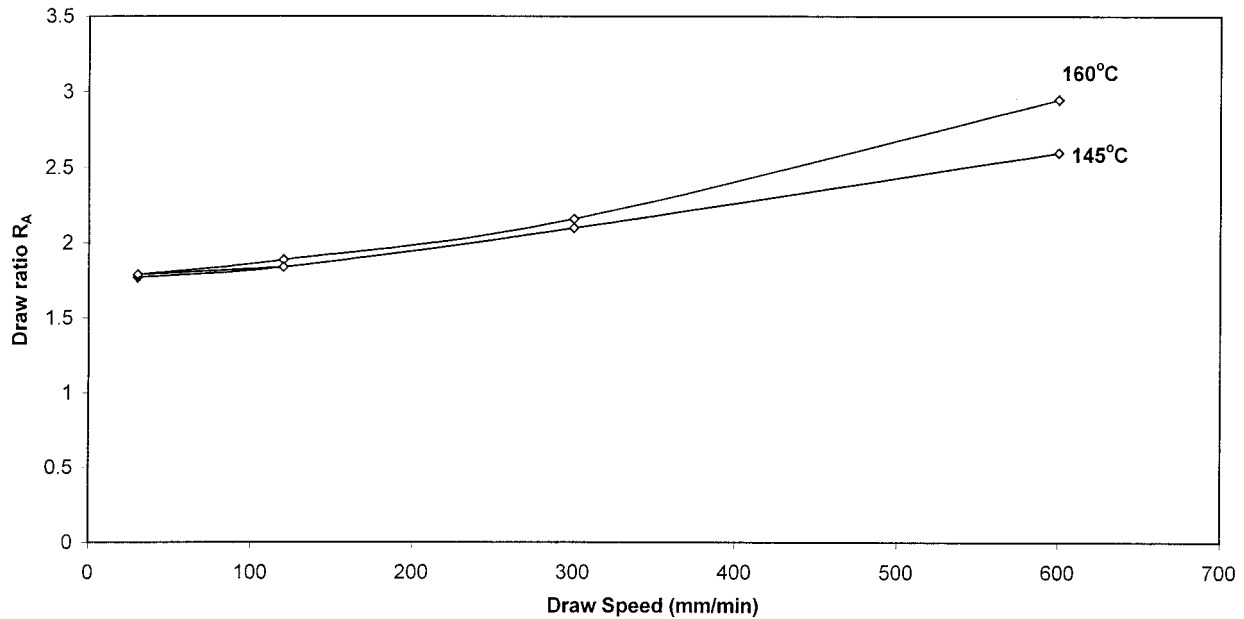


Figure 3 Variation of draw ratio R_A with draw speed for Delrin 150SA; $R_N = 1.7$; draw temperatures as indicated.

is caused. All measurements were performed at strain levels below 10^{-3} , and a high sample length/diameter ratio of 60 was maintained to minimize end effects.

Tensile strength was measured using an Instron with a specimen gauge length of 100 mm and a cross-head speed of 50 mm/min. Long flat grips with semi-circular grooves were used to clamp the sample. Most of the samples fractured away from the grips.

Dynamic three-point bend measurements were performed in bending mode at a frequency of 1 Hz using a Rheometrics Solids Analyzer RSA II (Rheometrics,

Poole, UK). The storage modulus and loss tangent were measured in the temperature range -100 to 150°C .

Thermal expansion measurements were made in the temperature range of -40 to 40°C , on equipment developed in this laboratory, described in detail previously.¹⁷

The melting behavior of the isotropic and die-drawn samples was studied using a Perkin-Elmer DSC 7 (Perkin Elmer Cetus Instruments, Norwalk, CT) equipped with Pyris software for data acquisition and

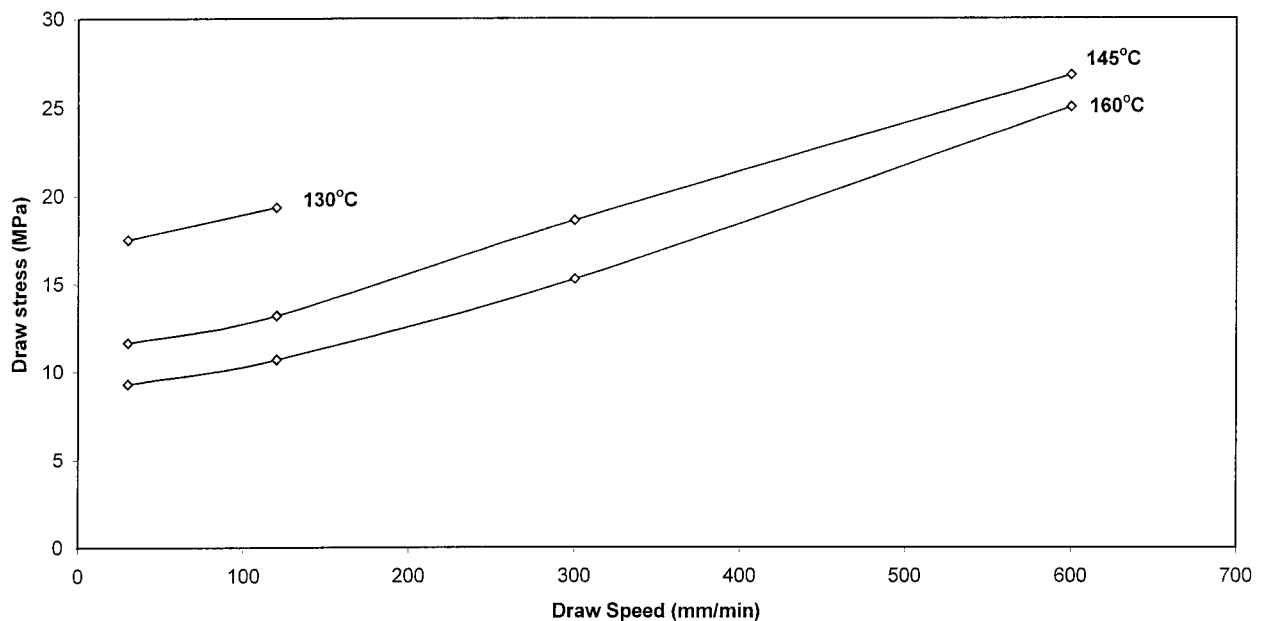


Figure 4 Variation of draw stress with draw speed for Delrin 150SA; $R_N = 1.7$; draw temperatures as indicated.

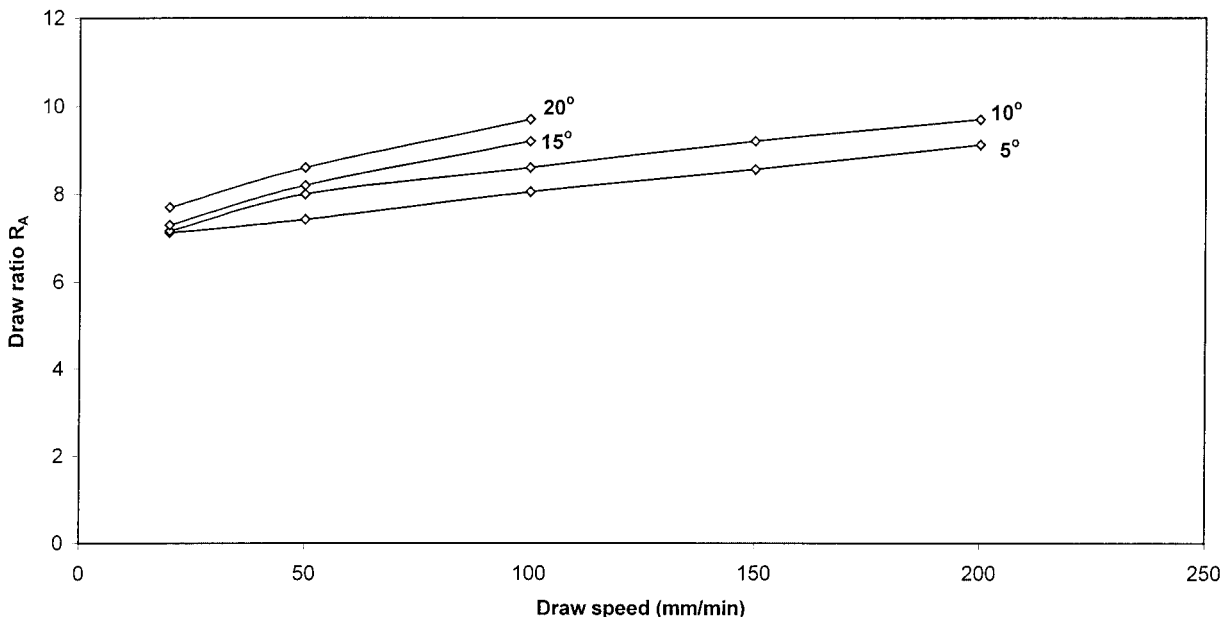


Figure 5 Effect of die angle on the variation of draw ratio R_A with draw speed. Delrin 150SA at draw temperature 160°C.

analysis. Indium (onset of melting 156.25°C and heat of fusion = 28.47 J/g) was used to calibrate the thermal response. The melting behavior of the draw ratio 7.9 sample was studied at different heating rates ranging from 5 to 100°C/min.

The wide-angle X-ray diffraction (WAXS) patterns of isotropic and drawn samples were taken using a flat-film camera with Cu- K_{α} radiation generated at 40 kV and 30 mA. Small-angle X-ray scattering (SAXS) patterns were obtained using the Siemens small-angle diffractometer (Hiltonbrooks Ltd., UK).

RESULTS AND DISCUSSION

Processing behavior

In previous studies of the tensile drawing and the die-drawing behavior of POM homopolymers, the optimum draw temperature was found to be in the region of 150°C.^{13,14} In the present work, the die-drawing behavior of POM was studied on a selection of billet R_N sizes drawn at different temperatures over a wide range of draw speeds. The results of the die drawing of Delrin 150SA rods at 160°C are shown in

Figures 1 and 2. The most prominent feature is that the actual draw ratio increases with the draw speed. In the case of a high R_N billet, the draw ratio increases rapidly and the product breaks at a low draw speed. Although drawing load in some cases falls slightly with draw speed, the drawing stress always increases.

The draw temperature has very little effect on the form of the draw ratio versus draw speed relationships. However, the draw stresses are substantially reduced with increasing temperature. The results for $R_N = 1.7$ are shown in Figures 3 and 4.

The effect of die angle was studied on the $R_N = 5.9$ billets of Delrin 150SA at a draw temperature of 160°C, results of which are shown in Figure 5. Higher die angles gave higher draw ratios at a given draw speed. The product draws down less beyond the die exit using the low-angle dies and the samples can be drawn at higher speeds.

At this stage in the investigation, a maximum draw ratio R_A of 12 was achieved at the draw speed of 100 mm/min, and a draw temperature of 160°C; this was disappointingly low.

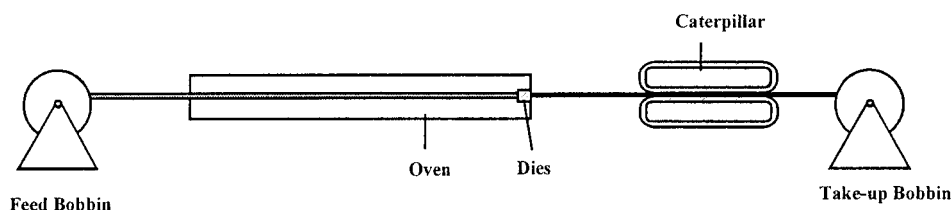


Figure 6 Schematic setup for the die-drawing of POM wire.

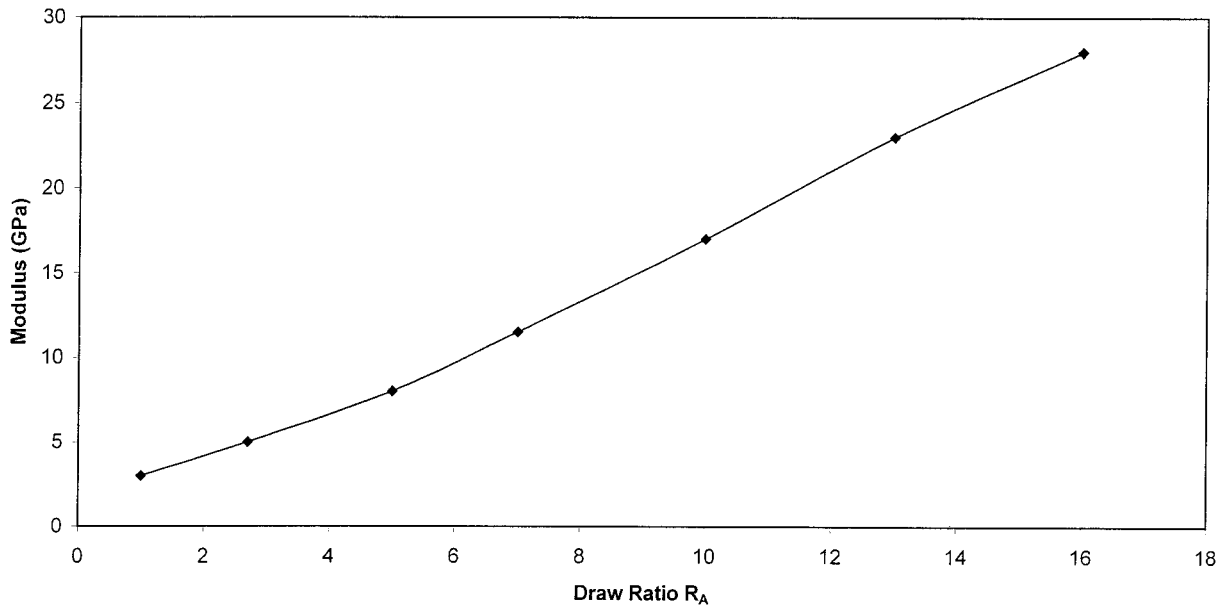


Figure 7 Variation of bending modulus with draw ratio R_A for Delrin 7031.

All the commercial rods of Delrin 150SA and Delrin 7031 had surface slip-stick extrusion marks. On drawing, failures were occurring on these marks. Some of these rods of Delrin 7031 were hand polished to remove these surface defects. A 10-cm-long tube was attached at the die exit and heated to the draw temperature of 160°C to assist further drawing beyond the die exit. A sample of draw ratio R_A of 7 could then be obtained by drawing the $R_N = 2.7$ billet up to the maximum available speed of 2000 mm/min. A draw ratio R_A of 14 was obtained through $R_N = 4.6$ up to the draw speed of 650 mm/min.

Work was carried out to improve extruded rod quality, and after some exploratory research a 7.5-mm rod was drawn through a 7-mm heated die to give a very smooth product. This rod was drawn through a 15° semiangle die of 3.2 mm exit diameter at 160°C. The die-drawing setup is shown in Figure 6. Lengths of 100 m, 2-mm diameter wire of draw ratio 11.5 were made at the draw speed of 1 m/min. Some redrawing experiments were carried out to improve the draw ratio and draw speed. A sample of draw ratio 3 was successfully redrawn through a die of $R_N = 2.5$ up to a draw speed of 2.5 m/min, to give a final draw ratio

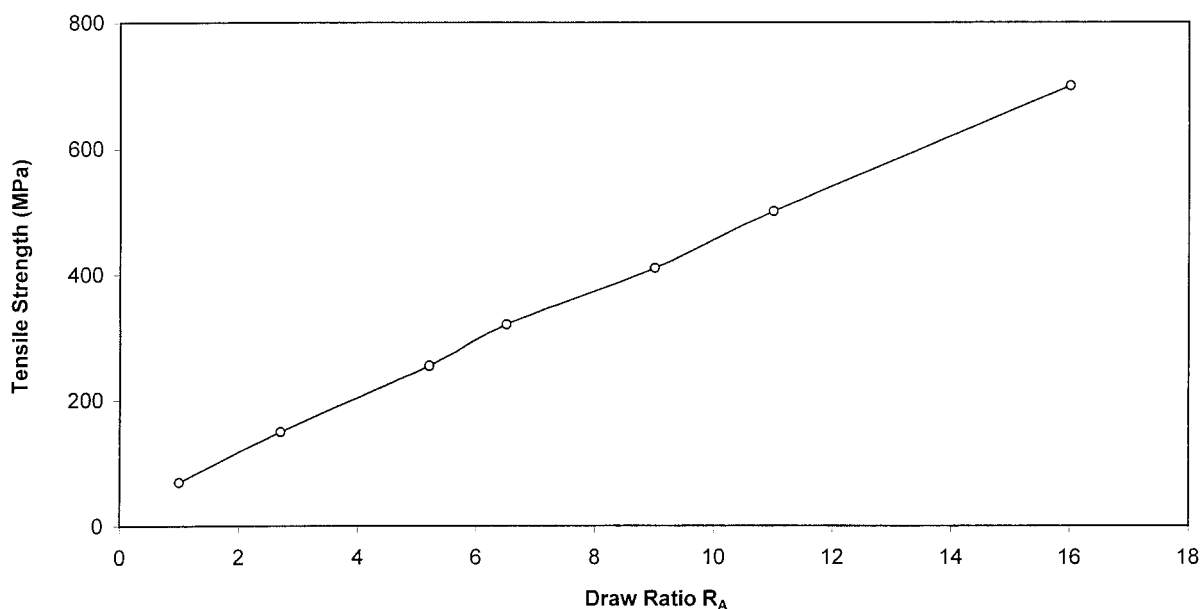


Figure 8 Variation of tensile strength with draw ratio R_A for Delrin 7031.

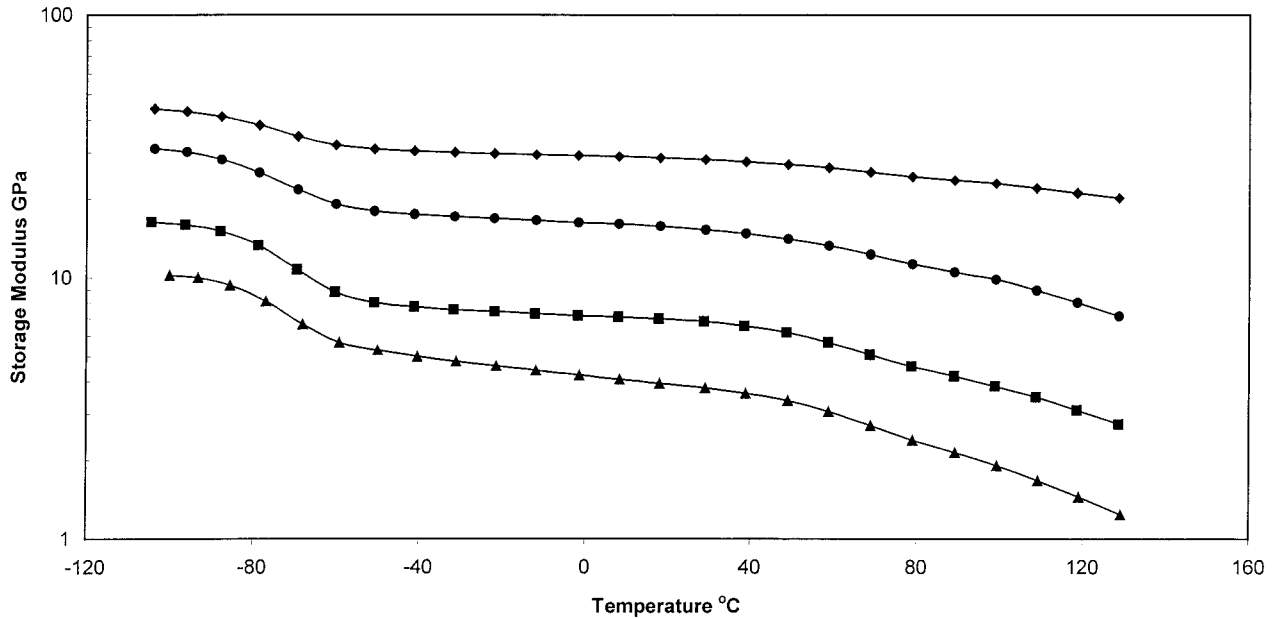


Figure 9 Temperature dependency of storage modulus E' for isotropic (\blacktriangle), $R_A = 4.1$ (\blacksquare), $R_A = 7.9$ (\bullet), $R_A = 15$ (\blacklozenge) for Delrin 7031.

of 11.5. Further redrawing of this drawn wire was not successful even at the low R_N of 1.2 die and at the high draw temperature of 170°C. On redrawing these samples of high draw ratio, fibers from the surface start peeling followed by a failure. It was possible to redraw the samples of up to draw ratio 5 to 6 through another die but the higher draw ratio samples could not be redrawn through a die. These samples of high draw ratio could be successfully redrawn by free-tensile drawing at elevated temperatures. Some sam-

ples of draw ratio 6–8 were freely drawn in a heated oven to give samples of draw ratio 16 to 18.

Visual examination of the die-drawn samples showed that these samples remained opaque up to the draw ratio of <3 and then became translucent between the draw ratio of 4 to 8. Above draw ratio 8, samples began to show some stress whitening, which increased rapidly with the draw ratio.

In the previous studies of die drawing, it was reported that the polymer left the wall of the die before

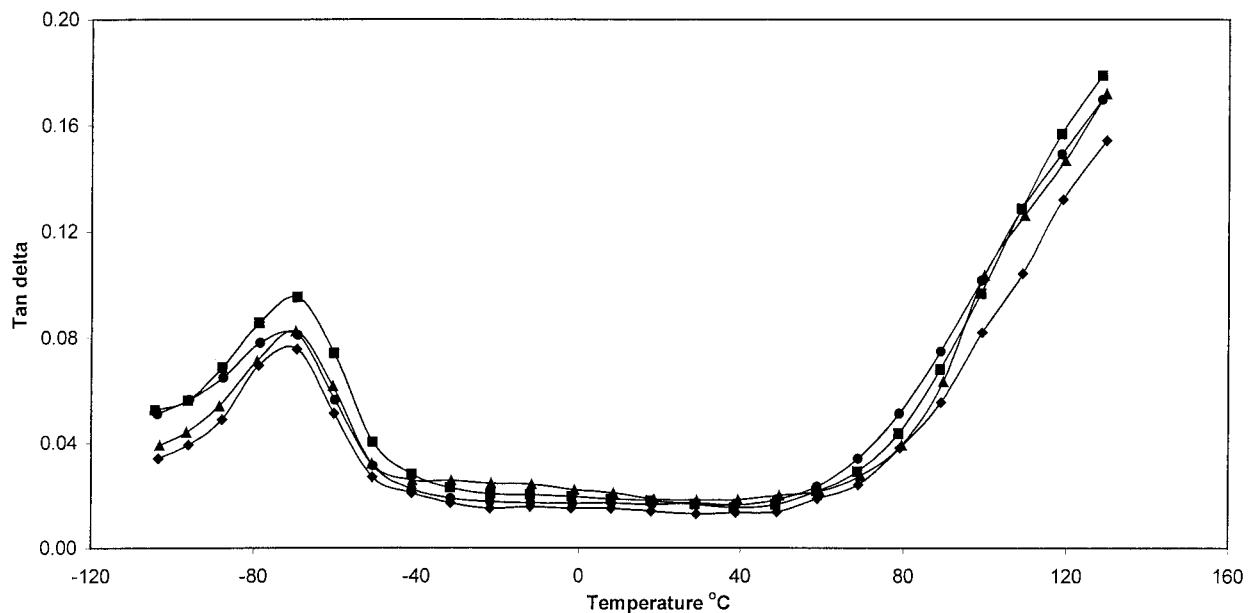


Figure 10 Temperature dependency of dynamic loss $\tan \delta$ for isotropic (\blacktriangle), $R_A = 4.1$ (\blacksquare), $R_A = 7.9$ (\bullet), $R_A = 15$ (\blacklozenge) for Delrin 7031.

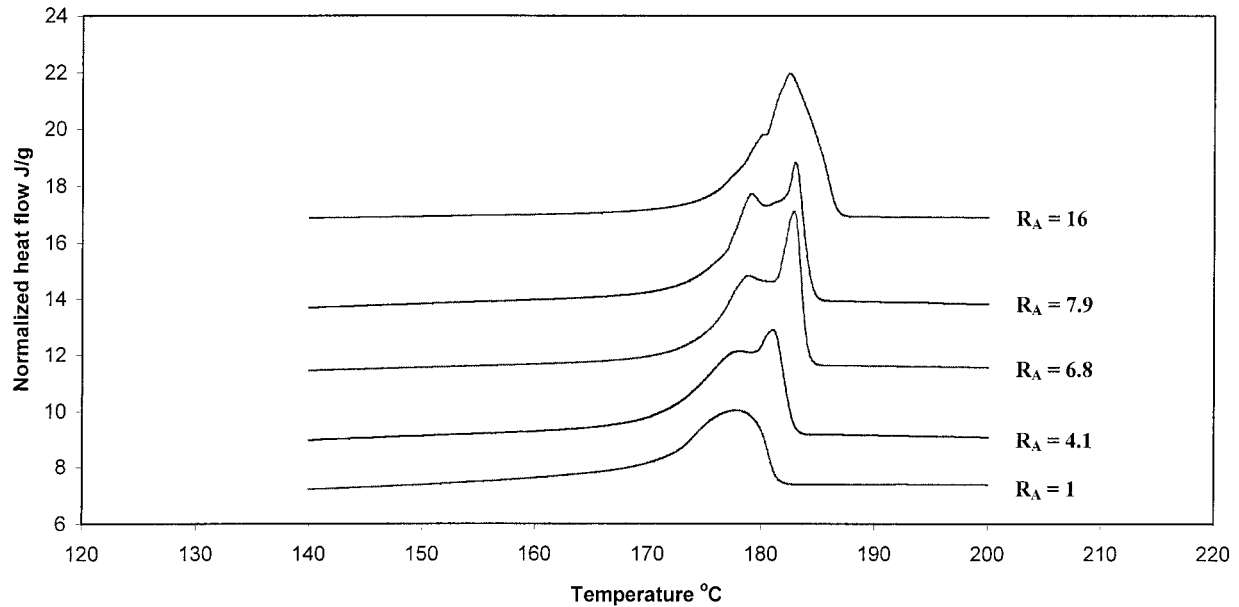


Figure 11 DSC thermographs of isotropic and drawn POM to draw ratios as indicated for Delrin 7031.

the die exit and followed an optimum strain and strain rate path.⁵⁻¹⁰ In these previous experiments conical dies with a semiangle of 15° were used, with a parallel land at the exit equal in length to the die exit diameter. Recently, theoretical analysis of the die drawing of rods suggested that the polymer does not leave the die wall in the conical region.¹⁸⁻²⁰ To verify this, dies were made without any land and drawing experiments were carried out using a video camera to monitor the product diameter at the die exit during the run. Conical dies of 5, 10, 15, and 20° semiangle were used and

the drawing was carried out at 150 and 160°C. The results showed that the drawn product diameter at the die exit was the same as the die exit diameter; hence, the material did not leave the die wall. It was observed that the product draws down rapidly immediately outside the die and then continues to draw down gradually until a constant diameter is reached. It was noticed that if the drawing is stopped and the load is removed, the material relaxes within the die. The profile of the cone of the extruded billet therefore did not match the die and gave the impression of material

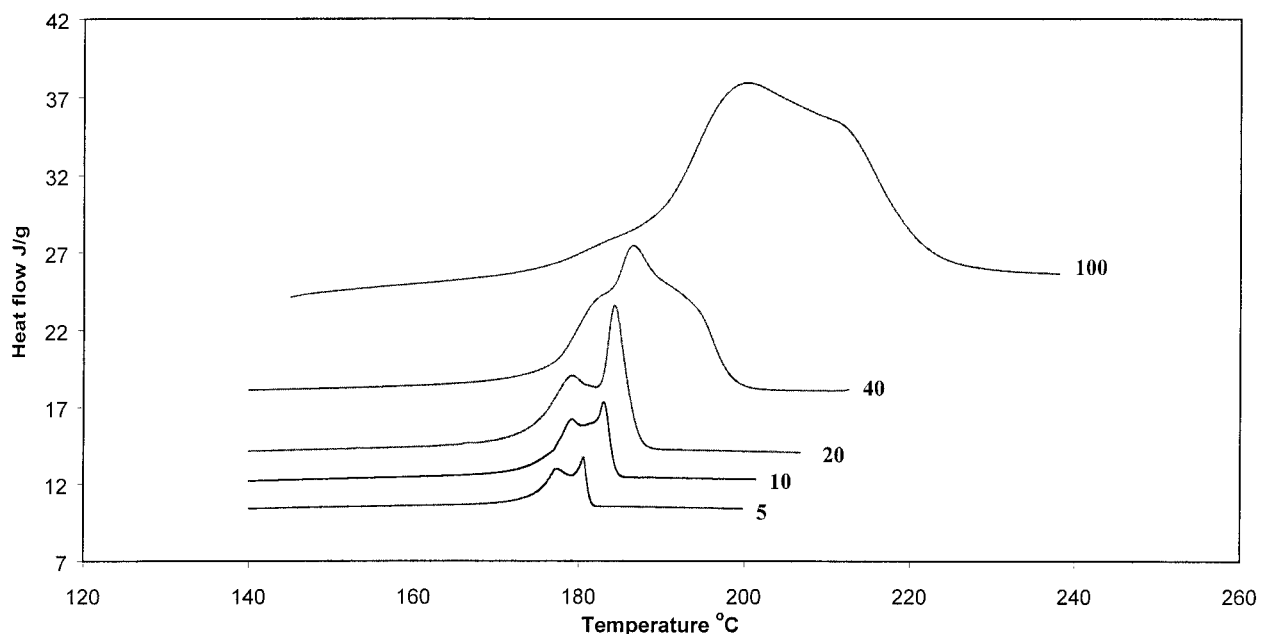


Figure 12 DSC thermographs of POM drawn to a draw ratio 7.9 at different heating rates (°C/min) as indicated for Delrin 7031.

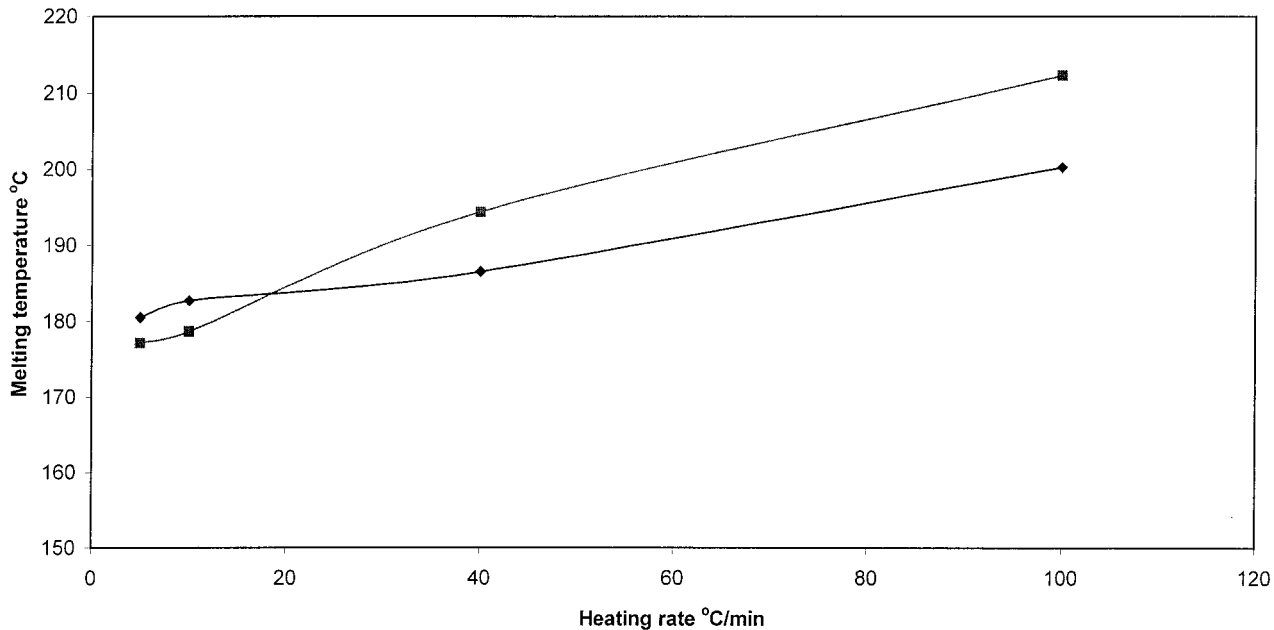


Figure 13 Effect of heating rate on the temperature of the double melting peaks of POM drawn to a draw ratio of 7.9: (■), shoulder peak; (◆), main melting endotherm for Delrin 7031.

leaving the die wall before the exit. The subsequent drawing down can be reduced or increased by cooling or heating the product beyond the die exit.

Mechanical properties

The bending modulus and the tensile strength of isotropic and drawn samples are shown in Figures 7 and 8, respectively. Modulus and tensile strength increase with increase in draw ratio, with a maxi-

mum bending modulus of 28 GPa and a maximum tensile strength of 700 MPa for a sample of draw ratio R_A of 16.

The dynamic storage modulus E' and $\tan \delta$ are shown as a function of temperature for draw ratios up to 9 in Figures 9 and 10, respectively. It can be seen that E' increases with draw ratio and that the temperature dependency of E' is significantly reduced at the higher draw ratios, so that E' does not change significantly from -70 to 70°C .

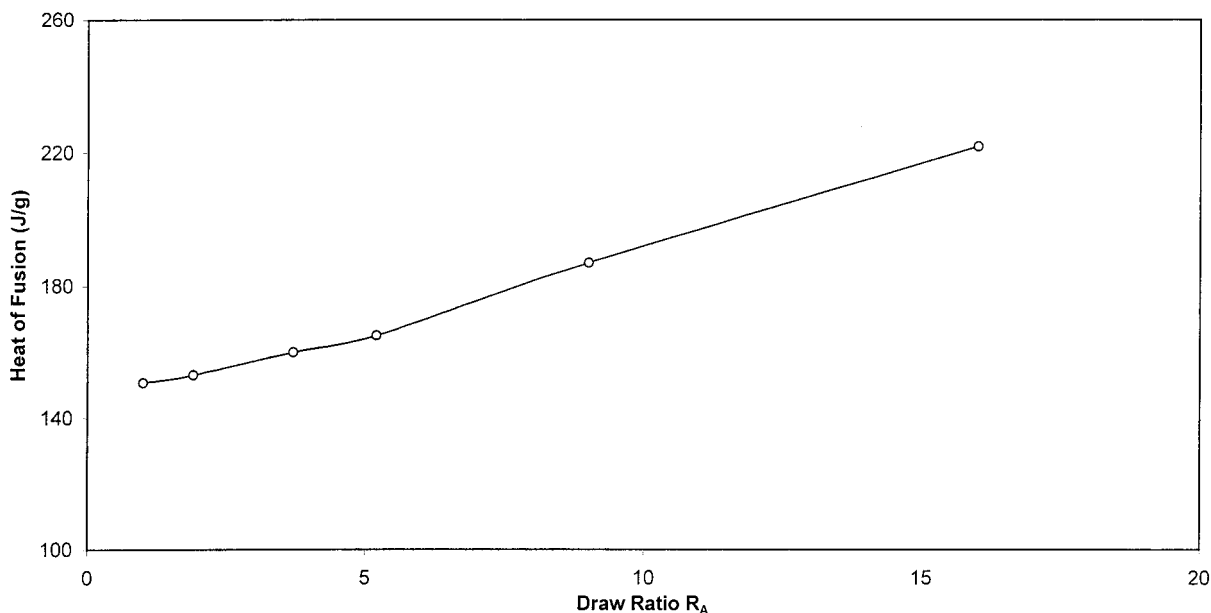


Figure 14 Variation of heat of fusion with draw ratio R_A for Delrin 7031.

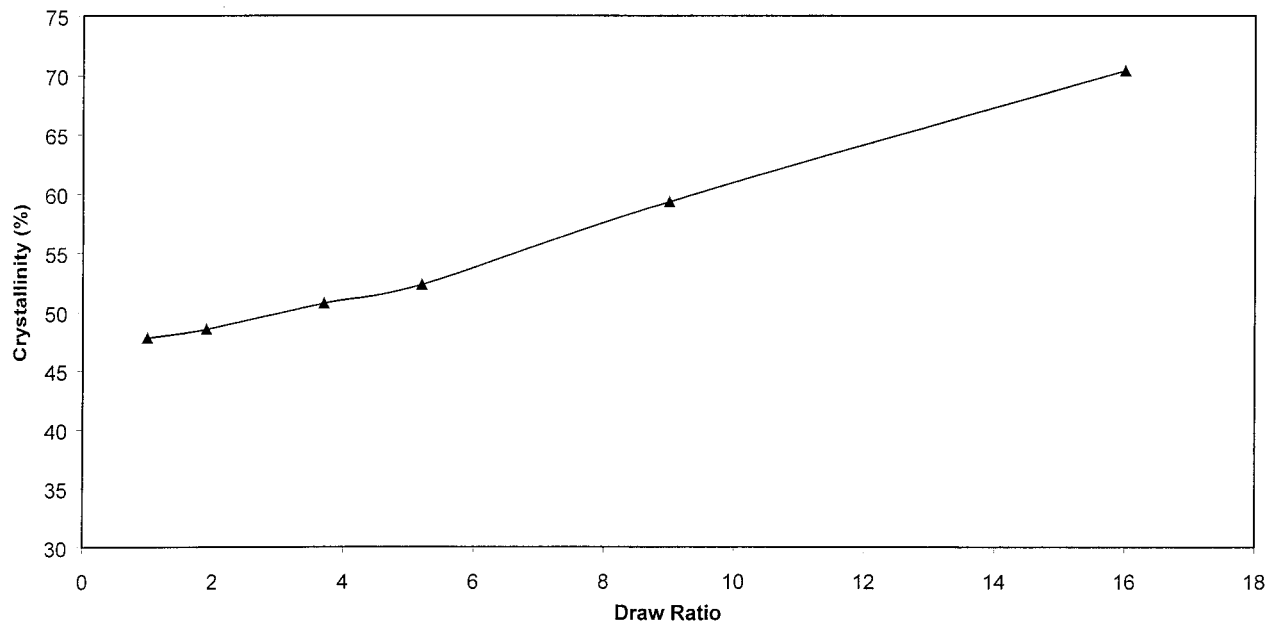


Figure 15 Variation of crystallinity with draw ratio R_A for Delrin 7031.

Tan δ shows a relaxation at -70°C , which is associated with main chain micro-Brownian motion in the amorphous regions.²¹ The tan δ peak is very much reduced for the highest draw ratio sample, suggesting that the molecular motion of amorphous chains is restricted in the drawn sample.

Melting behavior

The DSC endotherms of isotropic and drawn samples taken at a heating rate of $10^\circ\text{C}/\text{min}$ are shown in Figure 11. An isotropic sample gave a single melting peak at 177°C . At draw ratio 4, a second melting peak was observed at the lower temperature side of the high-temperature endotherm, slightly lower in temperature compared to that of isotropic material. With a further increase in draw ratio the low-temperature peak became sharp and the melting temperature increased to 182°C . Similar melting behavior was previously observed in the case of oriented polypropylene.²² Taraiya et al.²² and Yan et al.²³ attributed the strained noncrystalline region to the first melting peak and the extended folded chain blocks to the second melting peak at the higher temperature.

To confirm this interpretation, the draw ratio 7.9 sample was studied at different heating rates. The DSC endotherms are shown in Figure 12. It is evident that with increasing heating rate, the two peaks overlapped into one wide peak at a higher temperature than the two peaks. The effect of heating rate on the temperature of the double peaks is shown in Figure 13. Both peak temperatures increase because of the superheating effects. From the slopes of the curves, it

could also be inferred that the heating rate has a stronger effect on the first melting peak than on the second melting peak, indicating that the strained noncrystalline regions are associated with the low-temperature endotherm. This is in line with the observations of Taraiya et al.,²² Yan et al.,²³ and Clements et al.²⁴

The heat of fusion of these samples was found to increase with the increase in draw ratio. These results are shown in Figure 14. Crystallinity was determined from the heat of fusion calibrated with indium. The

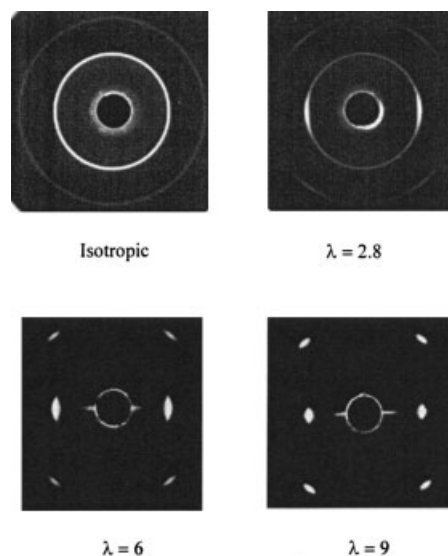


Figure 16 WAXD patterns for isotropic and die-drawn for Delrin 7031.

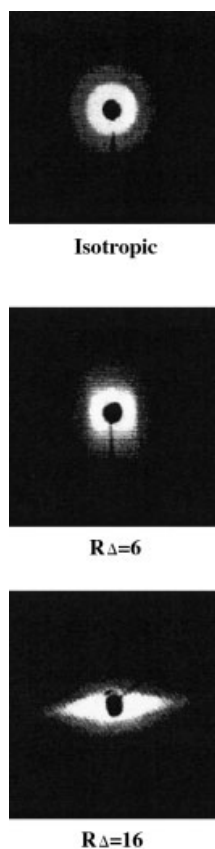


Figure 17 SAXS patterns for isotropic and die-drawn POM samples.

heat of fusion of POM crystal was set at 317.93 J/g.²⁵ Figure 15 shows that the crystallinity increases with the draw ratio.

Thermal expansion

The thermal expansion coefficient along the draw direction for POM reduces from $100 \times 10^{-6} \text{ }^\circ\text{C}^{-1}$ for the isotropic sample to $-1 \times 10^{-6} \text{ }^\circ\text{C}^{-1}$ for the sample of draw ratio 16. Similar results have been reported with highly drawn polyethylene.¹⁷

WAXD and SAXS

The WAXD patterns of the die-drawn samples of Delrin 150 are shown in Figure 16. The WAXD pattern obtained arises from the hexagonal unit cell with 9/5 helix of POM.²⁶ In the low draw ratio sample of 2.8, the (100) reflection consisted of a strong maximum on the equator and a weak ring. This suggests that in a majority of material the crystal *a*-axis is preferentially oriented perpendicular to the draw direction with a small portion of randomly oriented material. The intensity of the weak ring decreased with increase in draw ratio and disappeared at draw ratio 9. Qualita-

tively, it can be seen that the crystalline orientation is almost complete by the draw ratio of 9.

The SAXS patterns are shown in Figure 17. A two-point pattern was observed on the meridian for a sample of draw ratio 6. In a sample of draw ratio 16 a two-point pattern could not be seen, but the equatorial scattering attributed to microvoids was observed. Similar results were reported for the highly oriented polyethylene.²⁷

Isotropic polyoxymethylene has a spherulitic structure and, when it is drawn, this structure breaks up and transforms into a fibrillar structure by the draw ratio of 6–9. As the draw ratio is further increased, through a value of 9, SAXS studies show that the long period disappears and the crystalline orientation at this stage is almost complete. The disappearance of the long period is associated with the creation of many taut tie molecules producing a homogeneous structure, so that the electron density difference between amorphous and crystalline regions is much reduced. The further increase in the modulus beyond the draw ratio 9 is most probably associated with more and more tie molecules becoming taut. This is supported by the suppression of the $\tan \delta$ peak in the highly drawn sample.

CONCLUSIONS

A study of the die-drawing behavior of polyoxymethylene has shown that it is unlikely to achieve very high draw ratio samples at high commercially viable drawing speeds by single-stage die drawing. Redrawing experiments have shown that it is possible to produce intermediate draw ratio samples at high drawing speeds using multistage die drawing. These samples of intermediate draw ratio can be subsequently tensile drawn at elevated temperatures at a suitable strain rate to give high draw ratios.

References

1. Capaccio, G.; Ward, I. M. *Nat Physical Sci* 1973, 243, 143.
2. Ciferri, A.; Ward, I. M. *Ultra-High Modulus Polymers*; Applied Science Publishers: London, 1979.
3. Ward, I. M. *Adv Polym Sci* 1988, 70, 1.
4. Ward, I. M.; Coates, P. D.; Dumoulin, M. M. *Solid Phase Processing of Polymers*; Hanser: Munich, 2000; Chapter 9.
5. Coates, P. D.; Ward, I. M. *Polym Eng Sci* 1981, 21, 612.
6. Coates, P. D.; Ward, I. M. *Polymer* 1979, 20, 1553.
7. Gibson, A. G.; Ward, I. M. *Polym Eng Sci* 1980, 20, 1229.
8. Gibson, A. G.; Ward, I. M. *J Mater Sci* 1980, 15, 979.
9. Hope, P. S.; Richardson, A.; Ward, I. M. *J Appl Polym Sci* 1981, 26, 2879.
10. Taraiya, A. K.; Richardson, A.; Ward, I. M. *J Appl Polym Sci* 1987, 33, 2559.
11. Taraiya, A. K.; Nugent, M.; Sweeney, J.; Coates, P. D.; Ward, I. M. *Plast Rubber Compos Process Appl* 2000, 29, 46.

12. Hope, P. S.; Richardson, A.; Ward, I. M. *J Appl Polym Sci* 1981, 26, 2879.
13. Brew, B.; Ward, I. M. *Polymer* 1978, 19, 1338.
14. Coates, P. D.; Ward, I. M. *J Polym Sci Polym Phys Ed* 1978, 16, 2031.
15. Clark, E. S.; Scott, L. S. *Polym Eng Sci* 1974, 14, 682.
16. Richardson, A.; Parsons, B.; Ward, I. M. *Plast Rubber Compos Process Appl* 1986, 6, 347.
17. Orchard, G. A. J.; Davies, G. R.; Ward, I. M. *Polymer* 1984, 25, 1203.
18. Kukureka, S. N.; Craggs, G.; Ward, I. M. *J Mater Sci* 1992, 27, 3379.
19. Motashar, F. A.; Unwin, A. P.; Craggs, G.; Ward, I. M. *Polym Eng Sci* 1993, 33, 1288.
20. Mirza, M. S.; Taraiya, A. K.; Barton, D. C.; Ward, I. M., *IMEchE Proc Part E*, to appear.
21. Kaito, A.; Nakayama, K.; Kanesuna, H. *J Appl Polym Sci* 1986, 32, 3499.
22. Taraiya, A. K.; Unwin, A. P.; Ward, I. M. *J Polym Sci Polym Phys Ed* 1988, 26, 817.
23. Yan, R. J.; Jiang, B. *J Polym Sci Polym Phys Ed* 1993, 31, 1089.
24. Clements, J.; Zachmann, H. G.; Ward, I. M. *Polymer* 1988, 29, 1929.
25. Iguchi, M. *Makromol Chem* 1976, 177, 549.
26. Carazzolo, G. A. *J Polym Sci* 1963, A1, 1573.
27. Clements, J.; Jakeways, R.; Ward, I. M. *Polymer* 1978, 19, 639.